1521-0111/95/4/408–417$35.00
MOLECULAR PHARMACOLOGY

https://doi.org/10.1124/mol.118.115048
Mol Pharmacol 95:408–417, April 2019

Monod-Wyman-Changeux Allosteric Shift Analysis in Mutant $\alpha1\beta3\gamma2$L $GABA_A$ Receptors Indicates Selectivity and Crosstalk among Intersubunit Transmembrane Anesthetic Sites[S]

Andrea Szabo, Anahita Nourmahnad, Elizabeth Halpin, and Stuart A. Forman

Beecher-Mallinckrodt Laboratories, Department of Anesthesia Critical Care and Pain Medicine, Massachusetts General Hospital, Boston, Massachusetts

Received October 25, 2018; accepted January 19, 2019

ABSTRACT

Propofol, etomidate, and barbiturate anesthetics are allosteric coagonists at pentameric $\alpha1\beta3\gamma2$ $GABA_A$ receptors, modulating channel activation via four biochemically established intersubunit transmembrane pockets. Etomidate selectively occupies the two β^+/α^- pockets, the barbiturate photolabel R-5-allyl-1-methyl-5-(*m*-trifluoromethyl-diazirynylphenyl) barbituric acid (R-mTFD-MPAB) occupies homologous α^+/β^- and γ^+/β^- pockets, and propofol occupies all four. Functional studies of mutations at M2-15′ or M3-36′ loci abutting these pockets provide conflicting results regarding their relative contributions to propofol modulation. We electrophysiologically measured GABA-dependent channel activation in $\alpha1\beta3\gamma2$L or receptors with single M2-15′ (α1S270I, β3N265M, and γ2S280W) or M3-36′ (α1A291W, β3M286W, and γ2S301W) mutations, in the absence and presence of equipotent clinical range concentrations of etomidate, R-*m*TFD-MPAB, and propofol. Estimated open probabilities were calculated and analyzed using global two-state Monod-Wyman-Changeux models to derive log(d) parameters proportional to anesthetic-induced channel modulating energies (where d is the allosteric anesthetic shift factor). All mutations reduced the log(d) values for anesthetics occupying both abutting and nonabutting pockets. The Δlog(d) values [log(d, mutant) − log(d, wild type)] for M2-15′ mutations abutting an anesthetic's biochemically established binding sites were consistently larger than the Δlog(d) values for nonabutting mutations, although this was not true for the M3-36′ mutant Δlog(d) values. The sums of the anesthetic-associated Δlog(d) values for sets of M2-15′ or M3-36′ mutations were all much larger than the wild-type log(d) values. Mutant Δlog(d) values qualitatively reflect anesthetic site occupancy patterns. However, the lack of Δlog(d) additivity undermines quantitative comparisons of distinct site contributions to anesthetic modulation because the mutations impaired both abutting anesthetic binding effects and positive cooperativity between anesthetic binding sites.

Introduction

$GABA_A$ receptors are pentameric ligand-gated chloride channels and major inhibitory neurotransmitter receptors in the mammalian central nervous system (Olsen and Sieghart, 2009; Sigel and Steinmann, 2012). Intravenous general anesthetics including etomidate, propofol, and barbiturates act as allosteric coagonists at $GABA_A$ receptors, positively modulating GABA activation at low concentrations and directly activating receptors at high concentrations (Brohan and Goudra, 2017). These actions, assessed electrophysiologically, are quantitatively described by two-state Monod-Wyman-Changeux (MWC) models (Rüsch et al., 2004; Ruesch et al., 2012; Ziemba and Forman, 2016; Steinbach and Akk, 2019).

Genes for 19 different human $GABA_A$ receptor subunits have been identified: α1-6, β1-3, γ1-3, δ, ε, π, θ, and ρ1-3 (Olsen and Sieghart, 2009; Sigel and Steinmann, 2012). Each subunit contains a large extracellular domain, a transmembrane domain with four α-helices (M1–M4), and an intracellular domain between M3 and M4. Typical synaptic $GABA_A$ receptors contain α, β, and γ subunits arranged β-α-β-α-γ counterclockwise when viewed from the extracellular space, creating four types of subunit interfaces: α^+/β^-, α^+/γ^-, γ^+/β^-, and two β^+/α^- (Fig. 1) (Baumann et al., 2001; Phulera et al., 2018). Biochemical studies using photolabeling and substituted cysteine modification and protection have located receptor-bound anesthetics within intersubunit transmembrane pockets between M2 and M3 helices of one subunit ("+" faces) and M1 helices of adjacent subunits ("−" faces) (Forman and Miller, 2016; Nourmahnad et al., 2016). Etomidate and its analogs bind selectively to the two β^+/α^- outer transmembrane interfaces (Li et al., 2006) and the barbiturate photoprobe R-5-allyl-1-methyl-5-(*m*-trifluoromethyl-diazirynylphenyl) barbituric acid (R-*m*TFD-MPAB) binds selectively in homologous pockets at the α^+/β^- and γ^+/β^- interfaces (Chiara et al., 2013). Propofol and its analogs bind within all four pockets that etomidate and R-*m*TFD-MPAB inhabit, while these and other known anesthetics do not occupy the homologous

This work was supported by the National Institutes of Health National Institute of General Medical Sciences [Grant GM089745 to S.A.F.].
https://doi.org/10.1124/mol.118.115048.
[S] This article has supplemental material available at molpharm.aspetjournals.org.

ABBREVIATIONS: AN, anesthetics; c, ratio of GABA dissociation constants in open versus closed receptors; d, allosteric anesthetic shift factor; K_G, GABA dissociation constant for closed channels; L_0, basal receptor gating equilibrium (closed:open); MWC, Monod-Wyman-Changeux; P_{open}, open probability; PTX, picrotoxin; R-*m*TFD-MPAB, R-5-allyl-1-methyl-5-(*m*-trifluoromethyl-diazirynylphenyl) barbituric acid.

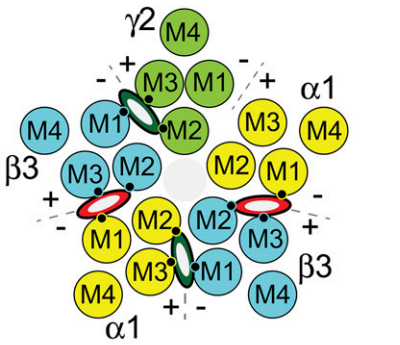

	M1	M2-15′	M3-36′
α1:	M236	S270	A291
β3:	L231	N265	M286
γ2:	L246	S280	S301

Fig. 1. Transmembrane residues abutting $GABA_A$ receptor anesthetic sites. The diagram depicts a cross section of a $\alpha1\beta3\gamma2L$ $GABA_A$ receptor through the transmembrane domain. The arrangement of the five subunits ($\alpha1$ = yellow; $\beta3$ = blue; $\gamma2$ = green) and the relative positions of the transmembrane helices (M1, M2, M3, and M4) is shown. Interfacial aspects of each subunit are labeled "+" (M3 side) or "−" (M1 side). Etomidate or propofol (red and white ovals) occupy the two β^+/α^- interfacial pockets and R-*m*TFD-MPAB or propofol (dark green and white ovals) occupy the corresponding α^+/β^- and γ^+/β^- pockets. The M1, M2, and M3 contact residues identified in the table below the diagram are depicted as small black circles. None of the three anesthetics bind in the α^+/γ^- interface. The table below the diagram identifies homologous M1, M2, and M3 residues on each type of subunit that abut intersubunit anesthetic sites. The effects of mutations at the M1 residues (34 residues before M2-15′) have been described previously (Nourmahnad et al., 2016).

α^+/γ^- interface (Jayakar et al., 2014; Forman and Miller, 2016; Nourmahnad et al., 2016).

The relative contributions of the distinct anesthetic sites to $GABA_A$ receptor gating modulation under drug occupancy conditions associated with general anesthesia remain uncertain. Of particular interest is whether the four sites where propofol binds differentially influence channel function. Conflicting results have emerged from functional studies of receptors with M2-15′ or M3-36′ mutations (Fig. 1) that impair anesthetic modulation (Mihic et al., 1997; Krasowski et al., 1998). Maldifassi et al. (2016) compared the effects of M2-15′ isoleucine substitutions on propofol modulation at GABA EC_5 in $\alpha1\beta2\gamma2L$ receptors, reporting that $\beta2$N265I nearly eliminated enhancement, while $\alpha1$S270I and $\gamma2$S280I produced negligible and small reductions, respectively, in propofol effects. These results suggest considerable asymmetry in energetic contributions from different propofol binding sites. Subsequently, Shin et al. (2018) used receptors formed from concatenated subunit assemblies and quantitative MWC analysis of currents directly activated by propofol, comparing the effects of $\beta2$M286W (M3-36′, β^+) and $\beta2$Y143W (β^-) mutations individually and in combination. In contrast to Maldifassi et al. (2016), Shin et al. (2018) reported approximately equal and additive effects of the four mutations, and suggested that up to six propofol sites might exist per receptor.

To gain more insight into the relative contributions of different anesthetic sites, we electrophysiologically assessed the effects of single mutations at M2-15′ and M3-36′ loci in $\alpha1$, $\beta3$, and $\gamma2L$ subunits in wild-type and mutant receptors expressed in *Xenopus* oocytes. We used MWC analysis to quantify shifts in channel gating energy (Feng et al., 2014) induced by equieffective concentrations of the β^+ site–selective anesthetic etomidate, the β^- site–selective barbiturate R-*m*TFD-MPAB, and propofol. We also tested whether the combined energy shifts associated with individual subunit mutations at M2-15′ or M3-36′ accounted for anesthetic effects in wild-type receptors.

Materials and Methods

Animals. Female *Xenopus laevis* frogs were used as a source of oocytes for electrophysiology. Frogs were housed in a veterinarian-supervised facility and oocyte harvest procedures were performed with approval from the Massachusetts General Hospital Institutional Animal Care and Use Committee, in accordance with state and federal regulations and the National Institutes of Health Office of Animal Care and Use recommendations.

Materials. DNA sequences encoding human $\alpha1$, $\beta3$, and $\gamma2L$ $GABA_A$ receptor subunits were cloned into pCDNA3.1 plasmids (Thermo Fisher Scientific). Etomidate at 2 mg/ml in sterile 35% propylene glycol:water was purchased from Hospira (Lake Forest, IL). Propofol (2,6-diisopropyl phenol, 99% purity) was purchased from Sigma-Aldrich (St. Louis, MO) and stored as a 100 mM stock in DMSO. R-*m*TFD-MPAB (99% pure) was a gift from Dr. Karol Bruzik (Deparment of Medicinal Chemistry and Pharmacognosy, Univerisity of Illinois, Chicago, IL) and stored in dark glass containers at −20°C as a 100 mM stock in DMSO. Anesthetics (AN) were diluted into electrophysiology buffer for experiments, with final DMSO <0.1%. All salts, buffers, and solvents were purchased from Sigma-Aldrich and were >98% pure.

Molecular Biology. We studied the effects of previously described mutations at M2-15′ and M3-36′ positions of $\alpha1$ ($\alpha1$S270I and $\alpha1$A291W) and $\beta3$ ($\beta3$N265M and $\beta3$M286W) and tryptophan mutations at the $\gamma2$ homologs ($\gamma2$S280W and $\gamma2$S301W). We have previously created three of these mutations (Scheller and Forman, 2002; Stewart et al., 2008; Desai et al., 2009). Oligonucleotide-directed mutagenesis with QuikChange kits (Agilent Technologies) was used to create mutations encoding $\alpha1$A291W, $\gamma2$S280W, and $\gamma2$S301W in the respective wild-type subunit expression plasmids. The presence of the desired mutations and absence of stray mutations were confirmed by sequencing through the entire cDNA sequence of each mutant plasmid.

Oocyte Expression of $GABA_A$ Receptors. Ovarian lobes were harvested from female *Xenopus* frogs under tricaine anesthesia. Defolliculated oocytes were prepared as previously described (Stewart et al., 2008). Oocytes were kept in ND96 (96 mM NaCl, 3 mM KCl, 1.8 mM $MgCl_2$, 1 mM $CaCl_2$, 5 mM Hepes, pH 7.4) at 17°C. Plasmids encoding wild-type and mutant subunits were linearized and used as templates for in vitro messenger RNA synthesis using commercial kits (Ambion Thermo Fisher). Messenger RNA transcripts were polyadenylated, purified, and stored in RNAase-free water at −80°C. Messenger RNA subunit mixtures in ratio $1\alpha{:}1\beta{:}5\gamma$ were microinjected into defolliculated oocytes (2–10 ng/oocyte).

Oocyte Electrophysiology. Oocytes were used in room temperature (20°C) two-microelectrode voltage-clamp electrophysiology experiments 24–96 hours after messenger RNA injection. Oocytes were placed in an open, low-volume (30 μl) flow chamber, and impaled with microelectrodes filled with 3 M KCl (<2 MΩ resistance). Superfusate solutions in ND96 were delivered to the flow chamber at 2 to 3 ml/min from glass syringe reservoirs via polytetrafluoroethylene tubing and valves and a micromanifold. Oocytes were voltage clamped at −50 mV (OC-725C; Warner Instruments, Hamden, CT). Amplified currents were low-pass filtered at 1 kHz, digitized (Digidata 1332; Molecular Devices, San Jose, CA), and recorded at 200 Hz on a computer running ClampEx version 8.0 software (Molecular Devices). Current traces were digitally filtered (low-pass 10 Hz) and baseline corrected using ClampFit version 8.0 software (Molecular Devices).

Spontaneous receptor activity was assessed in each receptor type by measuring picrotoxin (2 mM) inhibition of basal leak currents in the

absence of GABA, normalized to maximal GABA (0.1–3 mM) currents in the same oocytes (n = 3 oocytes for each receptor type). Maximal GABA efficacy was assessed by comparing maximal currents elicited with GABA alone to currents that were elicited by preapplication (15–30 seconds) of 3.2 μM etomidate, 8 μM R-mTFD-MPAB, or 5 μM propofol, followed by maximal GABA plus drug. Using the most effective of the three drugs, maximal GABA efficacy was calculated as the ratio of peak current elicited with high GABA alone to the drug-enhanced peak current.

GABA-dependent activation of receptors was assessed in the absence and presence of anesthetic solutions that equally modulate $\alpha1\beta3\gamma2$L receptor gating (approximately 2 × EC_{50} for loss-of-righting reflexes in tadpoles): 3.2 μM etomidate, 8 μM R-mTFD-MPAB, or 5 μM propofol (n = 3–5 oocytes per condition). Maximal control currents were assessed frequently (every other or third recording) to correct for variations over time in the number of functional receptors. Currents elicited with GABA (range: 0.01 μM to 3 mM) were normalized to the average of preceding and following maximal GABA (0.1–3 mM) controls recorded in the same cell. Currents elicited with GABA plus AN (no anesthetic preapplication) were also normalized to currents activated by maximal GABA without anesthetic, in the same cell. If pairs of sequential control currents differed by more than 10%, experiments done between these controls were excluded from analysis.

Estimated Open Probability Calculations. Estimated open probability (P_{open}), the fraction of active receptors in an experiment, was calculated from picrotoxin (PTX)-sensitive basal activity, maximal GABA efficacy, and experimental currents, all normalized to maximal GABA responses (Forman and Stewart, 2012). The calculation assumes that 2 mM picrotoxin inhibits all spontaneously active receptors (P_{open} = 0) and that maximum anesthetic-enhanced high GABA responses represent activation of all functional receptors (P_{open} = 1).

$$P_{open} = \frac{(I/I_{GABA}^{max}) + (I_{PTX}/I_{GABA}^{max})}{(I_{GABA+AN}^{max}/I_{GABA}^{max}) + (I_{PTX}/I_{GABA}^{max})} \quad (1)$$

where I/I_{max} is the normalized experimental current response; I_{PTX}/I_{max} is the mean normalized spontaneous activity; and $I_{GABA+AN}/I_{max}$ is the inverse of the mean maximal GABA efficacy.

Descriptive analysis of estimated P_{open} data was performed using nonlinear least-squares fits to a four-parameter logistic equation (GraphPad Prism 7; GraphPad Software Inc.):

$$P_{open} = \frac{P_{max} - P_{min}}{1 + 10^{[\log EC_{50} - \log(GABA)\cdot nH]}} + P_{min} \quad (2)$$

where EC_{50} is the half-activating GABA concentration, and nH is the Hill slope.

MWC allosteric shift analyses were performed in Origin 6.1 (OriginLab, Northampton, MA) as global fits to estimated P_{open} data both with and without anesthetic present. We previously described this method to quantify and compare allosteric gating shift factors (d) under identical anesthetic exposure conditions in $\alpha\beta\gamma$ and $\alpha\beta\delta$ $GABA_A$ receptors with dramatically different GABA efficacies (Feng et al., 2014). Here, we modified the approach by fitting log(d), a value proportional to the anesthetic-induced gating shift free energy, and thus suitable for energy additivity calculations. In these nonlinear least-squares fits, equieffective concentrations of the anesthetics are treated as a binary factor: 0 if no anesthetic is present, and 1 if present:where L_0 is the basal receptor gating equilibrium (closed:open), K_G is the GABA dissociation constant for closed channels; c is the GABA efficacy (ratio of dissociation constants in open/closed states; and $10^{[\log(d)]}$ = d is the allosteric anesthetic shift factor. The model assumes two equivalent GABA sites. When AN = 0, the right-hand part of the denominator equals 1 and eq. 3 simplifies to an MWC equation describing agonism by two equivalent GABA sites:

$$P_{open} = \frac{1}{1 + L_0 \times (\{[1 + (GABA)]/K_G\}/\{[1 + (GABA)]/cK_G\})^2 \cdot (\{[1 + (AN)]/10^{-6}\}/\{[1 + (AN)]/10^{\log(d)-6}\})} \quad (3)$$

$$P_{open} = \frac{1}{1 + L_0 \times (\{[1 + (GABA)]/K_G\}/\{[1 + (GABA)]/cK_G\})^2} \quad (4)$$

When AN = 1, eq. 3 closely approximates:

$$P_{open} = \frac{1}{1 + L_0 \times 10^{\log(d)} \times (\{[1 + (GABA)]/K_G\}/\{[1 + (GABA)]/cK_G\})^2} \quad (5)$$

Log(d) differences and sums of Δlog(d) calculations were performed in Microsoft Excel (Microsoft Corp., Redmond, WA) with propagation of errors (S.D.) as described by Bevington and Robinson (2002). Wild-type L_0 has been reported over a wide range between 1100 and 70,000 (Chang and Weiss, 1999; Rüsch et al., 2004; Ziemba and Forman, 2016). Fitted wild-type log(d) values, and thus calculated Δlog(d) values for mutant receptors, were insensitive to fixed wild-type L_0 values between 5000 and 50,000. We chose L_0 = 5000 for wild-type fits to eq. 3; L_0 for $\alpha1\beta3$N265M$\gamma2$L receptors was set at twice the wild-type value (10,000), based on previous results (Desai et al., 2009), and L_0 values for other mutants were set based on measured spontaneous open probabilities.

Statistical Analyses. The ratios of maximal GABA responses in the presence versus absence of anesthetic were compared with 1.0 using Student's t tests. Pairwise comparisons of fitted logistic parameters in the absence and presence of different anesthetics were performed using F tests in GraphPad Prism 7. For comparisons of log(d) values among different receptor types and different anesthetics, we calculated t statistics for the log(d) differences. The log(d) and S.E. values were derived using 48 or more individual data points fitted to an equation with three free parameters (eq. 3 with L_0 fixed), indicating at least 45 degrees of freedom, with $t > 2.02$ corresponding to $P < 0.05$; $P < 0.05$ was taken to indicate statistical significance.

Results

Receptor Characterization: Spontaneous Gating, GABA EC_{50}, and Maximal GABA Efficacy. We first characterized wild-type $\alpha1\beta3\gamma2$L and six mutant $GABA_A$ receptors for spontaneous activation and sensitivity to GABA using two-microelectrode voltage-clamp electrophysiology (Fig. 2; Table 1). Results in wild-type receptors (Table 1) were similar to previous reports (Nourmahnad et al., 2016). In the absence of GABA, we detected no picrotoxin-sensitive current in oocytes expressing $\alpha1\beta3\gamma2$L. Exposure to equihypnotic (2 × EC_{50}) anesthetic concentrations (3.2 μM etomidate, 5 μM propofol, or 8 μM mTFD-MPAB) activated wild-type receptors less than 1%. These anesthetic concentrations similarly enhanced maximal (1–3 mM) GABA responses by on average 14%, indicating that GABA alone activated approximately 88% of receptors.

All but one of the six mutant receptors conducted picrotoxin-sensitive current in the absence of GABA, indicating spontaneous

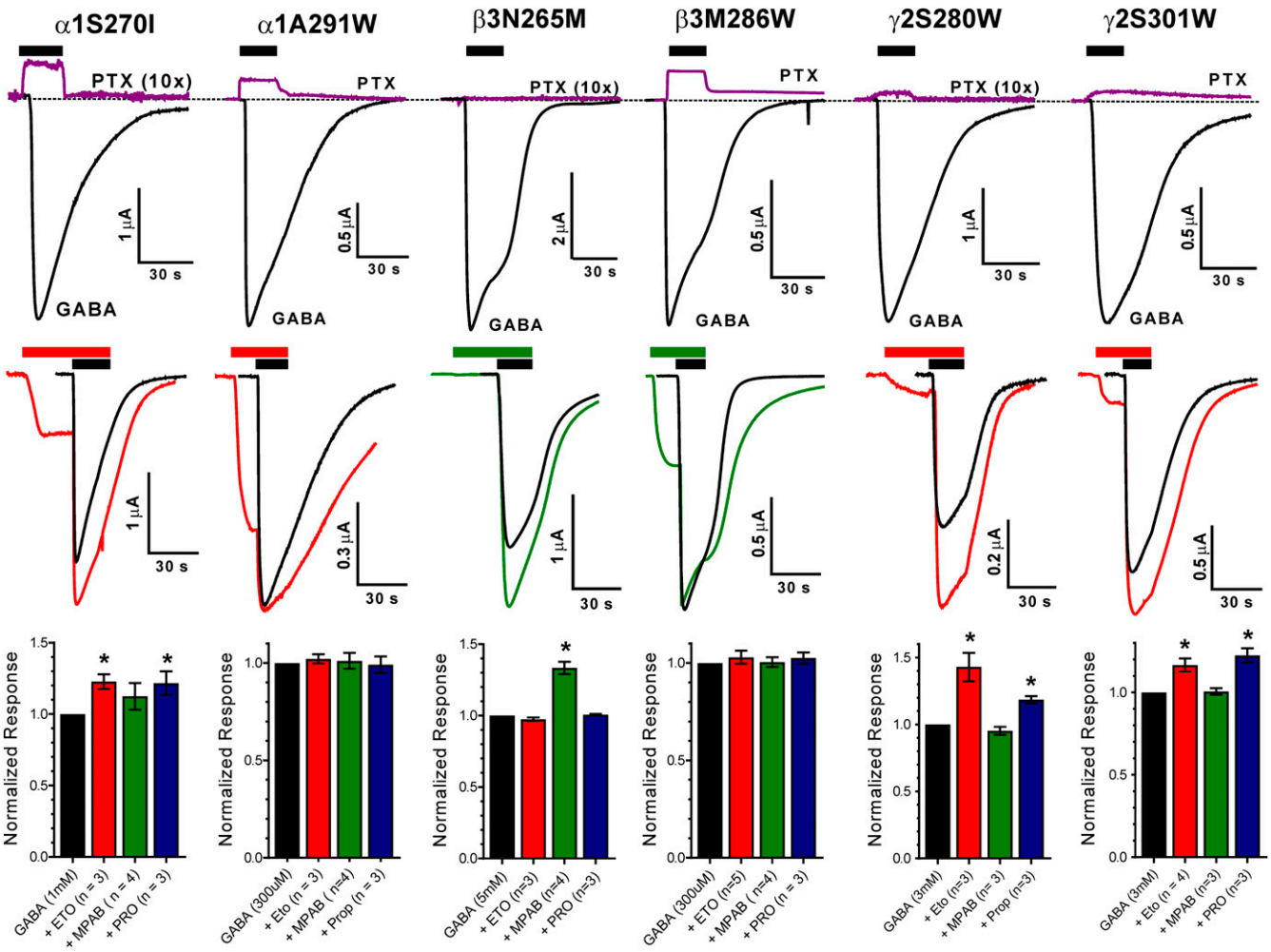

Fig. 2. Spontaneous activation and maximal GABA efficacy of mutant $GABA_A$ receptors. (Top row) Each panel displays current sweeps recorded from a single oocyte expressing $\alpha1\beta3\gamma2L$ receptors containing a single point mutation (labeled above the traces). The purple lines show currents before, during, and after 2 mM PTX application, while the black lines show currents activated with maximal GABA (0.3–3 mM). Drug applications are indicated by black bars above traces. Outward currents during PTX application represent inhibition of spontaneously active receptors. The PTX traces for α1S270I, β3N265M, and γ2S280W have been amplified 10-fold to better illustrate the effects. Average I_{PTX}/I_{GABA} ratios are summarized in Table 1. (Middle row) Each panel displays current sweeps recorded from a single oocyte expressing $\alpha1\beta3\gamma2L$ receptors containing a single point mutation (labeled above the traces). The black sweeps show currents activated with maximal GABA. Colored traces are currents recorded during 15–30 second pre-exposure to either 3.2 μM etomidate (red lines) or 8 μM R-*m*TFD-MPAB (green lines) followed by these drugs combined with maximal GABA. Anesthetic applications are indicated by colored bars and GABA applications by black bars above the traces. Note that currents are elicited by anesthetic alone in all but one mutant receptor, and that in four mutant receptors anesthetic also enhances maximal GABA responses. (Bottom row) Bars represent normalized ratios (mean ± S.D.; $n = 3$) of peak currents in the presence vs. absence of anesthetics (etomidate = red; R-*m*TFD-MPAB = green; propofol = blue). Increased maximal GABA currents in the presence of anesthetic drugs indicates that GABA alone activates less than 100% of functional receptors (* indicates $P < 0.05$). Maximal GABA efficacy for each mutant receptor is the inverse of the maximum ratio induced by the three drugs (Table 1).

gating (Fig. 2, top panels). No picrotoxin-sensitive currents were observed in oocytes expressing $\alpha1\beta3$N265M$\gamma2L$ receptors, consistent with previous results (Desai et al., 2009). The other M2-15′ mutants (α1S270I$\beta3\gamma2L$ and $\alpha1\beta3\gamma2$LS280W) consistently exhibited small (≤2% of maximal) picrotoxin-inhibited spontaneous currents (Table 1). All three M3-36′ mutants displayed over 5% spontaneous activation (Fig. 2; Table 1).

Anesthetic enhancement of maximal GABA responses varied among the mutant receptors (Figs. 2 and 3). None of the anesthetics enhanced maximal GABA activation of α1A291W$\beta3\gamma2L$ or $\alpha1\beta3$M286W$\gamma2L$ receptors, indicating GABA efficacies near 100%. Maximal GABA responses in all other mutant receptors were enhanced by at least one of the tested drugs (Fig. 2, middle and bottom panels). Current traces recorded for anesthetic enhancement of maximal GABA responses (Fig. 2, middle panels) also reveal the effects of anesthetic application alone before adding GABA. With the exception of $\alpha1\beta3$N265M$\gamma2L$ receptors, the anesthetic that best enhanced GABA responses also directly activated receptors when applied alone.

Gating and GABA sensitivity effects of most of the mutations that we studied are consistent with previous reports, most of which used different wild-type backgrounds (Krasowski et al., 1998; Ueno et al., 1999, 2000; Siegwart et al., 2003; Stewart et al., 2008; Desai et al., 2009). Two M3 mutations, α1A291W and β3M286W, display increased spontaneous channel gating, reduced GABA EC_{50}, and increased GABA efficacy (Table 1). These effects are all associated with stabilization of open relative to closed receptors (i.e., decreasing the L_0 parameter in two-state MWC models). Receptors with the M3 mutation γ2S301W also displayed spontaneous channel activation, but with GABA

TABLE 1
Functional characteristics of $GABA_A$ receptor mutants

Receptor	GABA EC_{50} [95% CI (n)]	GABA Efficacy ± S.D.	$I_{PTX}/I_{GABAmax}$ ± S.D.
	μM		
$\alpha1\beta3\gamma2L$	59 [53–66 (n = 3)]	0.88 ± 0.024 (n = 5)	<0.001 (n = 3)
M2-15′			
$\alpha1S270I\beta3\gamma2L$	2.3 [2.1–2.6 (n = 3)]	0.78 ± 0.054 (n = 6)	0.020 ± 0.0072 (n = 3)
$\alpha1\beta3N265M\gamma2L$	141 [128–156 (n = 3)]	0.75 ± 0.024 (n = 4)	<0.001 (n = 3)
$\alpha1\beta3\gamma2LS280W$	29 [24–35 (n = 4)]	0.70 ± 0.053 (n = 3)	0.015 ± 0.0043 (n = 3)
M3-36′			
$\alpha1A291W\beta3\gamma2L$	0.37 [0.27–0.52 (n = 3)]	0.99 ± 0.036 (n = 6)	0.10 ± 0.014 (n = 3)
$\alpha1\beta3M286W\gamma2L$	5.9 [4.5–7.7 (n = 4)]	0.96 ± 0.032 (n = 5)	0.061 ± 0.034 (n = 5)
$\alpha1\beta3\gamma2LS301W$	43 [32–58 (n = 3)]	0.84 ± 0.054 (n = 7)	0.078 ± 0.0088 (n = 3)

CI, confidence interval.

EC_{50} and GABA efficacy close to those of wild-type receptors (Table 1), as previously reported (Ueno et al., 1999). Receptors with α1S270I or γ2S280W mutations also displayed spontaneous activation together with low GABA efficacy. The α1S270I receptor reduced GABA EC_{50} about 10-fold relative to wild type (Ueno et al., 1999; Scheller and Forman, 2002), while γ2S280W is characterized by GABA EC_{50} only 2-fold lower than wild type. Receptors with β3N265M mutations exhibited no spontaneous activation and were characterized by reduced GABA efficacy and increased GABA EC_{50}, as previously reported (Siegwart et al., 2003; Desai et al., 2009).

Anesthetic Modulation of GABA-Dependent Receptor Activation. Figure 3 illustrates average GABA concentration-response relationships, calculated as estimated open probabilities (eq. 2 in *Materials and Methods*), which includes corrections for spontaneous activation and maximal GABA efficacy (Table 1). The wild-type ($\alpha1\beta3\gamma2L$) data demonstrate that all three anesthetics, at the equihypnotic concentrations used, similarly shifted GABA concentration-response curves to lower EC_{50} and increased maximum GABA efficacy. For the various mutant receptors, the patterns of anesthetic-induced changes in GABA concentration-response relationships varied, showing different degrees of direct activation (activation at 0 GABA), GABA EC_{50} shift, and increased GABA efficacy. Parameters from logistic fits to these GABA concentration-response curves with and without anesthetics are summarized in Supplemental Table 1.

Receptors with α1S270I or α1A291W mutations were modulated least by 8 μM R-*m*TFD-MPAB and most by 3.2 μM etomidate, while 5 μM propofol produced intermediate effects.

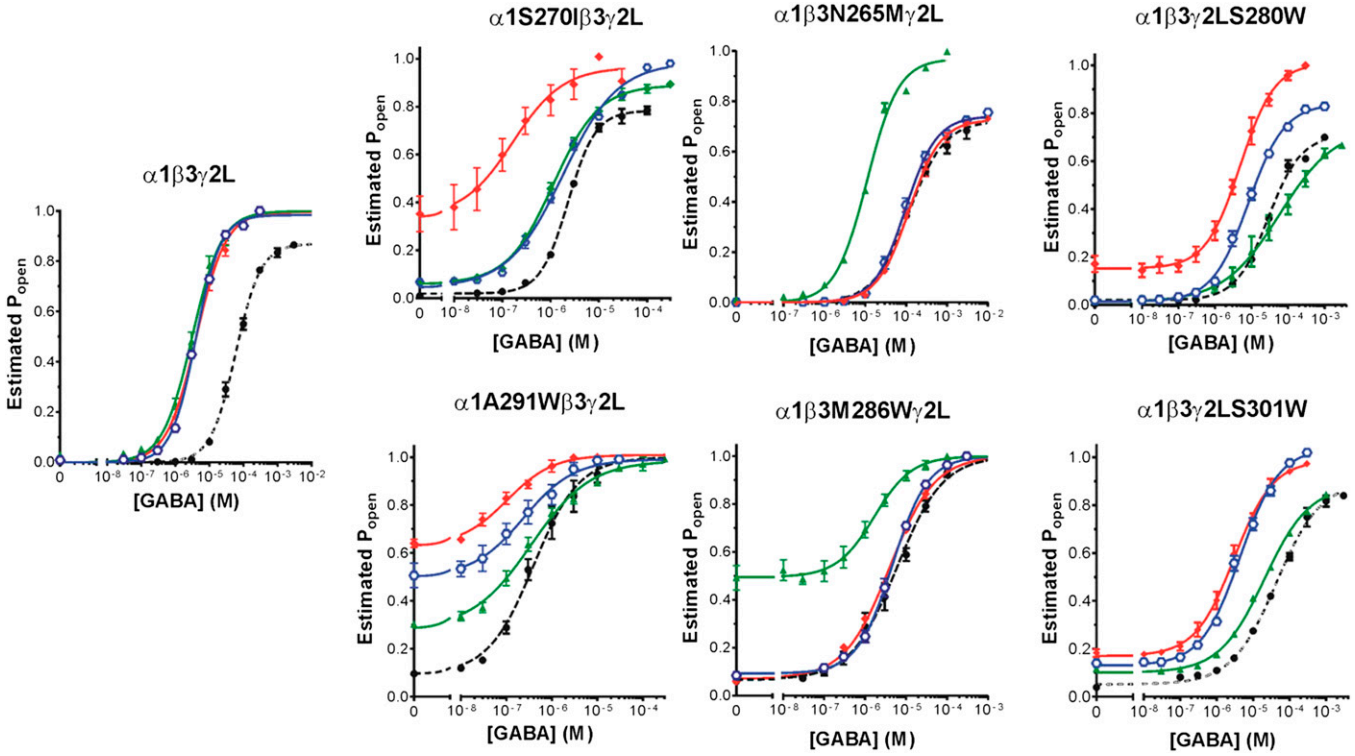

Fig. 3. Anesthetic effects on GABA-dependent activation of wild-type and mutant $GABA_A$ receptors. Each panel depicts estimated open probability (mean ± S.E.M.) calculated (eq. 1 in *Materials and Methods*) from normalized current responses ($n \geq 3$ per condition). Results for GABA alone are shown as solid black circles. Results for GABA plus anesthetic are shown as colored symbols: etomidate = solid red diamonds; R-*m*TFD-MPAB = solid green triangles; and propofol = blue hexagons. Lines through data points represent nonlinear least-squares fits to logistic functions (eq. 2 in *Materials and Methods*). Fitted logistic parameters are reported in Supplemental Table 1.

In contrast, receptors with either β3N265M or β3M286W mutations were most strongly modulated by R-*m*TFD-MPAB, but weakly or unaffected by etomidate and propofol. Receptors with γ2S280W or γ2S301W mutations both displayed anesthetic modulation patterns similar to that in α1S270I$\beta3\gamma2$L receptors. Both mutants were modulated most by etomidate, least by R-*m*TFD-MPAB, and displayed intermediate sensitivity to propofol.

Some of our observations conflicted with prior reports describing these mutations, perhaps due to different wild-type backgrounds or experimental designs. We observed over 75% reduction of propofol log(d) in α1S270I$\beta3\gamma2$L receptors ($P < 0.001$), while Maldifassi et al. (2016) reported EC_5 modulation in α1S270I$\beta2\gamma2$L similar to that in wild-type $\alpha1\beta2\gamma2$L. Another earlier study by Krasowski et al. (1998) reported moderately less propofol modulation at GABA EC_5 in α2S270Iβ1 receptors than in $\alpha2\beta1$. In receptors formed from concatenated subunit assemblies containing two β2M286W mutant subunits, Shin et al. (2018) fitted $L_0 > 10{,}000$, while our experiments revealed 6% spontaneous activity (Table 1), corresponding to $L_0 = 17$ (Table 2), which is consistent with our previous results (Stewart et al., 2008). Shin et al. (2018) also reported that propofol agonist efficacy was reduced less than 50% in the β2M286W double mutant, while we observed that β3M286W mutations nearly obliterated propofol modulation. Krasowski et al. (1998) also reported obliteration of propofol modulation in $\alpha2\beta1$M286W$\gamma2$ receptors, but also reported direct activation by high propofol concentrations. We did not examine the effects of high propofol concentrations in this study.

Allosteric Shift Analyses. Allosteric two-state equilibrium MWC coagonist models of anesthetic actions in $GABA_A$ receptors assume the presence of two equivalent GABA sites and account for GABA-dependent activity with three parameters (eq. 4 in *Materials and Methods*): the basal closed:open gating equilibrium (L_0); the GABA dissociation constant for closed receptors (K_G); and GABA efficacy, i.e., the ratio of GABA dissociation constants in open versus closed receptors (c). Anesthetic effects, including receptor activation at zero GABA (direct activation), reductions in GABA EC_{50}, and increased maximal GABA efficacy are all attributed to allosteric coagonism, which depends on anesthetic concentration, the number of anesthetic sites, and anesthetic affinities for closed versus open receptor states (Rüsch et al., 2004; Ruesch et al., 2012; Steinbach and Akk, 2019). For MWC allosteric shift analyses at equieffective anesthetic concentrations (established in wild-type receptors), we collapsed all of the aforementioned anesthetic factors into a single fitted parameter, log(d) (eqs. 3 and 5, *Materials and Methods*). An important advantage of allosteric shift analysis over fitting MWC efficacy from anesthetic-dependent activation is that for receptors with unmeasurable spontaneous activation (e.g., wild type), log(d) values are insensitive to L_0, which is uncertain under these conditions. In our MWC shift analyses, we performed sensitivity tests by constraining L_0 over a range from 50,000 to 5000, resulting in narrow log(d) parameter ranges for etomidate (−1.92 to −1.96), R-*m*TFD-MPAB (−2.13 to −2.18), and propofol (−1.89 to −1.95); in contrast, the log of fitted GABA efficacies, 2log(c), in these same calculations ranged from −5.44 to −4.42 as L_0 dropped 10-fold from 50,000 to 5000.

Figure 4 illustrates this approach in wild-type $\alpha1\beta3\gamma2$L and the three M2-15′ mutant receptors. Each row of panels illustrates estimated P_{open} results in the absence (black circles)

TABLE 2

Fitted parameters from Monod-Wyman-Changeux allosteric shift analysis

Values were derived from nonlinear least-squares fits with eq. 3 (*Materials and Methods*) with L_0 constrained (three dependent parameters), to pooled P_{open} estimates. At least 48 values of P_{open} from experiments at eight or more GABA concentrations, with and without anesthetics, in at least three different oocytes were used in each calculation. Figure 4 displays both data and fitted models.

Mutation	L_0	Etomidate (3.2 μM)			R-*m*TFD-MPAB (8 μM)			Propofol (5 μM)		
		$K_G \pm$ S.D.	c ± S.D.	Log(d) ± S.D.	$K_G \pm$ S.D.	c ± S.D.	Log(d) ± S.D.	$K_G \pm$ S.D.	c ± S.D.	Log(d) ± S.D.
		μM			μM			μM		
Wild type	5000	90 ± 13	0.0061 ± 0.00040	−1.91 ± 0.075	100 ± 13	0.0059 ± 0.00037	−2.13 ± 0.065	90 ± 11	0.0061 ± 0.00035	−1.89 ± 0.065
α1S270I	60	4.0 ± 0.65	0.064 ± 0.00047	−1.58 ± 0.043	3.1 ± 0.46	0.071 ± 0.0043	−0.42 ± 0.036	4.0 ± 0.69	0.065 ± 0.0049	−0.44 ± 0.039
β3N265M	10,000	110 ± 10	0.0065 ± 0.00021	−0.024 ± 0.023	90 ± 20	0.0068 ± 0.0041	−1.49 ± 0.078	110 ± 10	0.0066 ± 0.00023	−0.09 ± 0.023
γ2S280W	100	31 ± 4.1	0.068 ± 0.0033	−1.21 ± 0.042	25 ± 4.1	0.070 ± 0.0041	0.16 ± 0.041	18 ± 2.7	0.076 ± 0.0036	−0.39 ± 0.037
α1A291W	10	1.1 ± 0.24	0.09 ± 0.012	−1.22 ± 0.038	1.0 ± 0.35	0.10 ± 0.019	−0.49 ± 0.071	1.3 ± 0.47	0.09 ± 0.019	−0.93 ± 0.055
β3M286W	17	14 ± 4.5	0.08 ± 0.014	−0.22 ± 0.094	18 ± 6.5	0.07 ± 0.016	−1.20 ± 0.045	16 ± 5.1	0.07 ± 0.013	−0.20 ± 0.085
γ2S301W	15	27 ± 7.3	0.14 ± 0.014	−0.72 ± 0.054	43 ± 8.2	0.14 ± 0.010	−0.25 ± 0.053	28 ± 8.3	0.14 ± 0.015	−0.64 ± 0.062

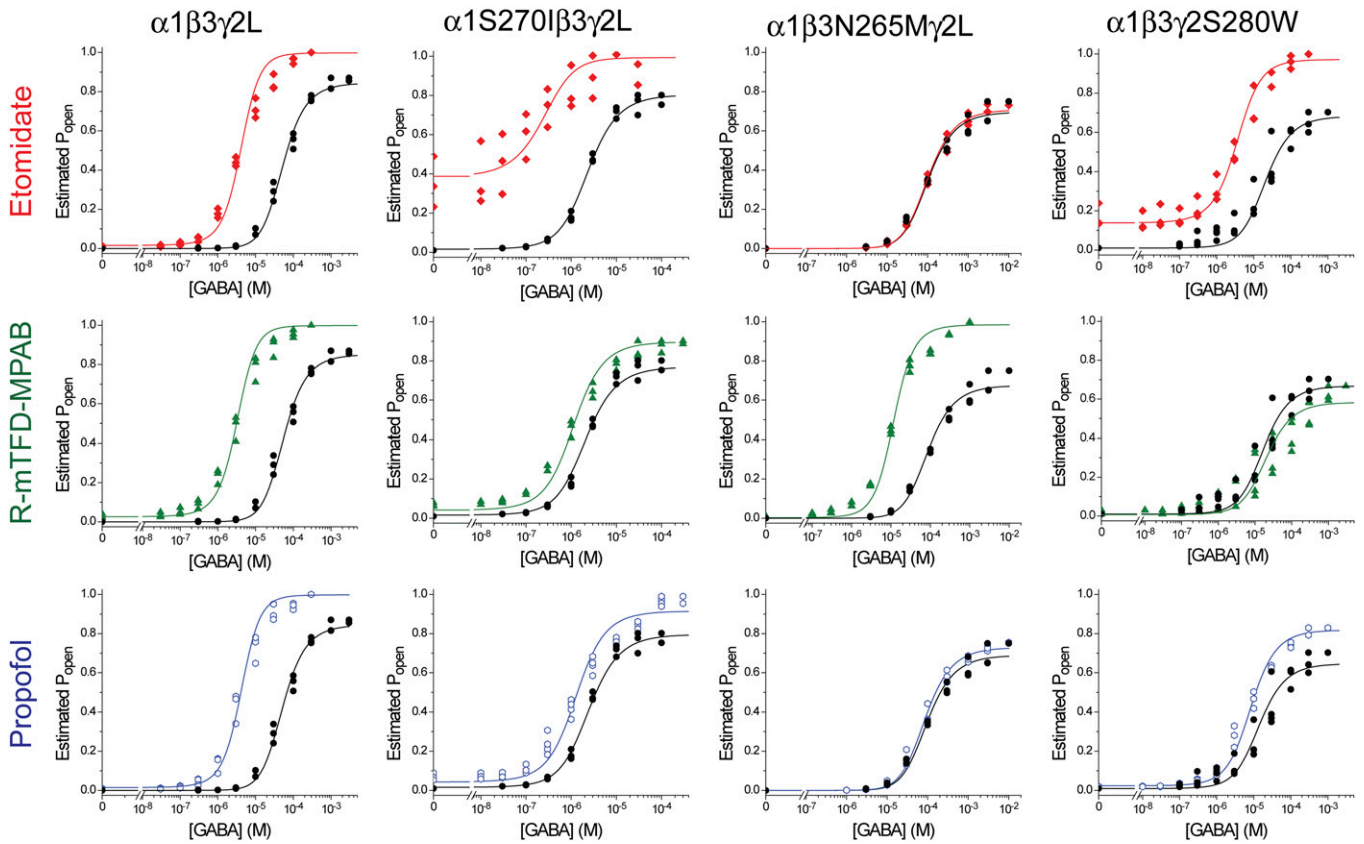

Fig. 4. Anesthetic-induced Monod-Wyman-Changeux allosteric shifts in wild-type and M2-15′ mutant $GABA_A$ receptors. Each panel displays estimated open probability data points (the same data as in Fig. 3) for one type of receptor (identified by labels above columns) and the effects of one equieffective anesthetic solution (identified by labels to the left of rows). Lines through data points represent nonlinear least-squares fits to eq. 3 in *Materials and Methods* with L_0 fixed and three free parameters: two that describe GABA responses and one, log(d), that quantifies anesthetic effects on gating. Lines were plotted using separate equations for GABA alone (eq. 4 in *Materials and Methods*; black lines) or GABA plus anesthetic (eq. 5 in *Materials and Methods*; colored lines). The L_0 values and fitted parameters are reported in Table 2.

versus presence of a single anesthetic (colored symbols). Both control GABA concentration-response relationships and the effects of anesthetics were well-fitted ($R^2 > 0.94$) by the MWC allosteric shift equation (eq. 3 in *Materials and Methods*; solid lines in Fig. 4 panels).

Table 2 summarizes the MWC fitted parameters for Fig. 4 and for the MWC fits for M3-36′ mutants (data not shown). Notably, the values for K_G and c varied little among nonlinear least-squares fits in the same receptor with different anesthetics, serving as internal consistency checks on the method. The parameters that varied the most among fits for each type of receptor were the log(d) values characterizing the allosteric gating shifts produced by different anesthetics. Figure 5 illustrates all of the fitted log(d) values for comparison within and between different drugs and receptors.

Mutant-associated log(d) shifts [Δlog(d) values, Table 3] are directly proportional to the differences between wild-type and mutant receptors in gating free energy shifts produced by the standardized equieffective anesthetic concentrations [ΔΔG = ΔG(mutant) − ΔG(wild type)]. We hypothesized that the mutated sites independently and additively contributed to anesthetic modulation, predicting that the sum of the Δlog(d) values for mutations on all three subunit types would approximately account for wild-type effects (Forman, 2012). However, summing all Δlog(d) values for M2-15′ or M3-36′ mutant effects for each drug resulted in totals that were consistently much larger than the wild-type log(d) values (Table 3; $t > 11$; $P < 0.05$ for both). We reasoned that the mismatch between mutant sums for the Δlog(d) and wild-type log(d) values might be due to inclusion of both local steric and allosteric effects of mutations in the calculations. Assuming that the Δlog(d) values for α^+ and γ^+ mutations with etomidate and β^+ mutations with R-*m*TFD-MPAB represent purely allosteric effects, we subtracted these from the propofol Δlog(d) values to estimate residual local mutant effects. However, the adjusted sums for both M2-15′ and M3-36′ mutations still differed from the wild-type log(d) for propofol (Table 3, right-most column). The sum of adjusted Δlog(d) values for the M2-15′ mutants, which produced small allosteric effects, exceeded the wild-type log(d) value ($t = 6.2$; $P < 0.05$), while that for M3-36′ mutants, which produced large allosteric effects, was below the wild-type log(d) value ($t = 3.5$; $P < 0.05$).

Discussion

We used point mutations and MWC model–based analysis, aiming to quantify the energetic contributions of distinct $GABA_A$ receptor anesthetic sites to channel gating, and to test whether these account for wild-type modulation. Two previous studies used similar approaches, exploiting β^+/α^- interfacial site mutations that reduce anesthetic modulation.

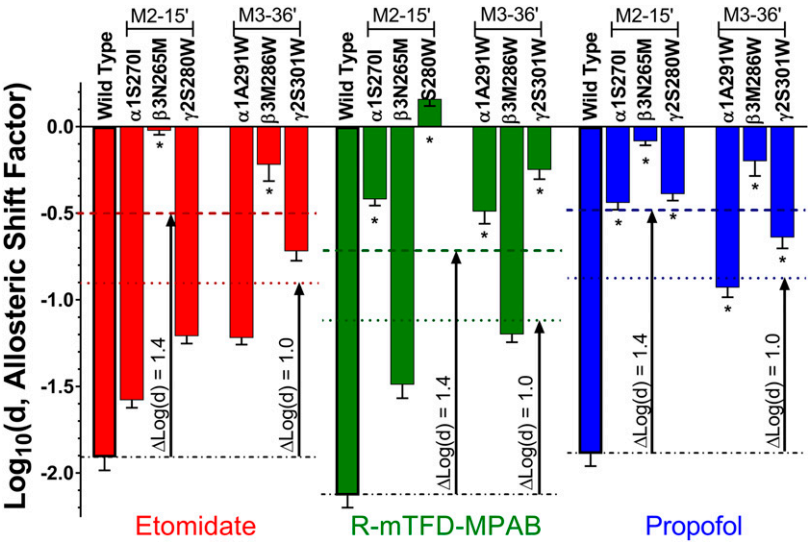

Fig. 5. Summary of anesthetic allosteric shift parameters. Each bar represents a fitted log(d) value (mean ± S.D.) for one of the three equieffective anesthetic solutions in one of the seven types of $GABA_A$ receptors included in this study. Bars are color coded according to anesthetic (red = 3.2 μM etomidate; green = 8 μM R-*m*TFD-MPAB; blue = 5 μM propofol) and labeled with the corresponding receptor type. Mutants are grouped into M2-15′ and M3-36′ subgroups. Asterisks (*) indicate mutations at loci that are adjacent to the anesthetic's binding sites, based on biochemical studies.

Guitchounts et al. (2012) used $GABA_A$ receptors formed from concatenated $\beta1$-$\alpha2$ and $\beta1$-$\alpha2$-$\gamma2$ assemblies, comparing $\Delta\Delta\log(\text{GABA EC}_{50})$ values for etomidate modulation in wild-type receptors versus receptors with $\alpha1$M236W mutant dimers, trimers, or both. The summed energy shifts for dimer and trimer mutants matched the difference between wild-type and double-mutant receptors. More recently, Shin et al. (2018) used MWC analysis of propofol agonism in $GABA_A$ receptors containing one to four propofol site tryptophan mutations. Assuming that each mutation obliterated one site, their results were consistent with independent, additive, and approximately equal gating energies per site. Additionally, MWC analyses of wild-type receptor activation with pairs of modulators that act via distinct sites provide more evidence of independent and additive energy contributions (Li et al., 2013, 2014; Shin et al., 2017, 2019). Thus, we hypothesized that independence and additivity are general features of anesthetic modulator sites.

Our approach for quantifying mutation-induced changes in anesthetic modulation had several advantages over earlier studies. Using GABA-dependent activation data, MWC shift analysis accounts for anesthetic activation at 0 GABA, reduced GABA EC_{50}, and increased GABA efficacy with a single parameter, log(d), that is proportional to gating energy change and suitable for additivity tests. This approach is clearly superior to assessing anesthetic effects at a single low GABA concentration (e.g., EC_5). Shifts in log(d) are also superior to $\Delta\log(\text{GABA EC}_{50})$ calculations because MWC analyses of P_{open} estimates correct for both spontaneous channel gating (Stewart et al., 2008; Germann et al., 2018) and maximal GABA efficacy in receptor variants (Feng et al., 2014). Our approach is similar in theory to the MWC analysis of direct anesthetic agonism by Shin et al. (2018), but also avoids using high potentially inhibitory drug concentrations. Sensitivity tests also showed that log(d) is insensitive to the L_0 parameter in wild-type analyses, while MWC efficacy values derived from direct agonism data are strongly dependent on L_0 (Germann et al., 2018).

To evaluate the utility of MWC shift analyses in this study, we used both etomidate, which binds selectively to β^+/α^- transmembrane sites, and R-*m*TFD-MPAB, which binds selectivity to homologous α^+/β^- and γ^+/β^- sites. Previous

TABLE 3

Additivity of ΔLog(d) values for M2 and M3 mutations by drug

Values for wild type are log(d) ± S.D. from fits of eq. 3 (*Materials and Methods*) to estimated P_{open} data (see Fig. 4; Table 2). Values for mutant receptors represent differences between log(d) values for wild type and mutants.

Mutation	ΔLog(d) (Mutant − Wild Type) ± S.D.			
	Etomidate	*m*TFD-MPAB	Propofol	Propofol (Adjusted)[a]
Wild type	−1.91 ± 0.075	−2.13 ± 0.065	−1.89 ± 0.065	−1.89 ± 0.065
M2-15′				
$\alpha1$S270I	0.33 ± 0.086*	1.71 ± 0.074	1.45 ± 0.076	1.12 ± 0.11
$\beta3$N265M	1.89 ± 0.078	0.64 ± 0.10*	1.81 ± 0.069	1.17 ± 0.12
$\gamma2$S280W	0.70 ± 0.086*	2.29 ± 0.077	1.50 ± 0.075	0.80 ± 0.11
Sum (x − 1)	−2.9 ± 0.15	−4.6 ± 0.15	−4.8 ± 0.13	−3.1 ± 0.20
M3-36′				
$\alpha1$A291W	0.69 ± 0.084*	1.6 ± 0.96	0.96 ± 0.085	0.27 ± 0.12
$\beta3$M286W	1.7 ± 0.12	0.93 ± 0.079*	1.7 ± 0.11	0.76 ± 0.13
$\gamma2$S301W	1.19 ± 0.092*	1.88 ± 0.084	1.25 ± 0.091	0.06 ± 0.13
Sum (x − 1)	−3.6 ± 0.17	−4.5 ± 0.15	−3.9 ± 0.16	−1.1 ± 0.22

[a]Adjusted propofol Δlog(d) values were calculated by subtracting presumed allosteric mutant effects based on etomidate and R-*m*TFD-MPAB experiments (identified by an asterisk in each mutant row) from unadjusted propofol Δlog(d) values.

studies showed that β3N265M and β3M286W mutations obliterate etomidate sensitivity (Belelli et al., 1997; Stewart et al., 2008), so we expected mutations in α^+/β^- and γ^+/β^- pockets to minimally affect etomidate modulation. Conversely, we anticipated that α^+ and γ^+ mutations would impair modulation by R-*m*TFD-MPAB, while β^+ mutations would produce minimal effects. Indeed, for both etomidate and R-*m*TFD-MPAB, ranking of Δlog(d) values for α, β, and γ mutations at either M2-15′ or M3-36′ reflects their biochemically established site selectivity (Fig. 5; Table 3). Etomidate modulation was affected far less by α1 and γ2 mutations than by β3 mutations. Correspondingly, R-*m*TFD-MPAB modulation was reduced far more by γ2 and α1 mutations than by β3 mutations. Our analysis also suggests that for R-*m*TFD-MPAB, the γ^+/β^- site mediates a larger effect than the α^+/β^- site, as previously suggested (Chiara et al., 2013; Jayakar et al., 2015). Within subunits, M2-15′ mutations consistently impaired modulation more than M3-36′ mutations for anesthetics that bind in adjacent sites (Table 3).

For propofol, every mutation reduced log(d) by at least 50%, with Δlog(d) values ranked β3N265M > β3M286W > α1S270I $\approx$ γ2S280W > γ2S301W > α1A291W (Fig. 5; Table 3). This outcome is consistent with biochemical evidence that propofol binds in all of the sites we studied (Chiara et al., 2013; Jayakar et al., 2014). The larger Δlog(d) values for β3 mutations probably reflect two β^+/α^- sites per receptor versus the single propofol sites altered by α1 or γ2 mutations. However, assuming that each β^+/α^- site contributes one-half of the propofol Δlog(d) associated with β3N265M (Table 3), then each β^+/α^- site contributes less than α^+/β^- or γ^+/β^- sites. Similar analysis for β3M286W suggests that all four propofol sites contribute comparably to channel modulation [Δlog(d) range -0.85 to -1.25 per site]. However, we cannot assume that these mutations all completely prevented adjacent anesthetic binding. Analysis of multiple mutations at each position might strengthen such comparisons.

Log(d) analysis (Fig. 5; Table 2) further demonstrated that every mutation reduced the modulating effects of drugs that bind in nonadjacent sites (all at $P < 0.05$). With etomidate, α^+ or γ^+ mutations reduced log(d) by up to 60% from wild type. Similarly, β3 mutations reduced log(d) for R-*m*TFD-MPAB by up to 43%. Interestingly, M3-36′ mutations affected nonadjacent anesthetics more than M2-15′ mutations in the same subunit. Considering all log(d) results together with biochemically established site occupation patterns for each drug (Figs. 1and 5) reveals that M2-15′ mutations abutting anesthetic sites reduce log(d) by at least 75% [i.e., Δlog(d) > 1.4], while nonabutting M2-15′ mutations reduce log(d) by less than 50% [i.e., Δlog(d) < 1.0]. The M3-36′ mutant effects do not discriminate as clearly between adjacent and nonadjacent sites. For example, γ2S301W induces Δlog(d) > 1.0 for etomidate, but is nonabutting, and both α1A291W and γ2S301W induce Δlog(d) < 1.4 for propofol.

In contrast to Guitchounts et al. (2012) and Shin et al. (2018), we found that the sum of mutant Δlog(d) values on all three subunits consistently exceeded log(d) for wild type (Table 3). This observation diverges from the expectation that mutant effects in distinct sites are local, independent, and energetically additive. Instead, it appears that the mutations also reduced cooperative linkages that reinforce concerted subunit state transitions, which may involve rearrangements of structured water in the anesthetic binding pockets. Alternatively, mutations may have promoted previously unseen inhibitory effects when both etomidate and R-*m*TFD-MPAB sites are occupied (Jayakar et al., 2015), or even the two R-*m*TFD-MPAB sites, because each α^+ or γ^+ mutation reduced log(d) for the barbiturate by well over 50%. The mutations also could have enhanced anesthetic inhibition, but current traces (e.g., Fig. 2, middle panels) showed no relief-of-inhibition surge currents.

Most mutations we studied also reduced the MWC efficacy of GABA (inversely proportional to c in Table 2). The exception is β3N265M, which also induces no spontaneous activation. This suggests that reduced MWC agonist efficacies, both orthosteric and allosteric, may be associated with spontaneously gating mutant receptors (Germann et al., 2018). However, correcting Δlog(d) for log(c) does not fully reconcile wild-type anesthetic effects with summed mutant shifts (Supplemental Table 2). Also, M2-L9′ mutations are counterexamples in which spontaneous activation is apparently unaccompanied by reduced GABA or anesthetic efficacy in MWC analyses (Chang and Weiss, 1999; Scheller and Forman, 2002; Rüsch et al., 2004).

To summarize, quantitative MWC analyses showed that M2-15′ and M3-36′ mutations substantially reduce $GABA_A$ receptor modulation by anesthetics that bind in both adjacent and nonadjacent intersubunit pockets. The ranked effects of M2-15′ mutations correlated with biochemically established anesthetic site occupancy patterns, validating prior studies (Mihic et al., 1997; Krasowski et al., 1998; Walters et al., 2000; Maldifassi et al., 2016). In comparison, the effects of hydrophobic mutations at M3-36′ and on M1 helices (Nourmahnad et al., 2016) do not reliably discriminate between adjacent and nonadjacent anesthetics. Generalizing from these results, mutant function analyses have limited value for identifying transmembrane drug contact residues, whereas approaches based on covalent modification (e.g., photolabeling or substituted cysteine modification and protection) provide strong steric inferences when applicable (Forman, 2018). Surprisingly, previously reported energy additivity among distinct anesthetic sites (Guitchounts et al., 2012; Shin et al., 2018) is not supported by our current results, complicating quantitative comparisons of different propofol binding sites. Our additivity analysis implies that mutations impaired both adjacent anesthetic binding effects and allosteric crosstalk between sites that underlies cooperativity among anesthetics in wild-type receptors. Interestingly, previous comparison of the two β^+/α^- sites using α1M236W mutations in concatenated subunit assemblies (Guitchounts et al., 2012) found equal and additive etomidate effects, while another using β3N265M mutations found unequal etomidate but equal propofol effects (Maldifassi et al., 2016). Thus, different mutations may divergently affect symmetry and/or crosstalk among anesthetic sites. Energy additivity in wild-type $GABA_A$ receptors is supported by studies of drug combinations (Shin et al., 2017; Cao et al., 2018) that notably used receptors formed from concatenated subunit assemblies. Concatenated receptors display less spontaneous activation than free subunit assemblies, and may also reduce heterogeneity in subunit arrangement (Baumann et al., 2001; Guitchounts et al., 2012). Indeed, bulky mutations located at subunit interfaces could disrupt receptor assembly. Studies evaluating the combined energetic effects of etomidate and R-*m*TFD-MPAB in wild-type $GABA_A$ receptors formed from both free and concatenated subunits are needed for

comparison with our current results. Finally, while two-state MWC models of $GABA_A$ receptor function have proven remarkably useful for describing the effects of drugs and mutations, they do not account for multiple closed, open, desensitized, and blocked receptor states that could be differentially affected by these factors.

Acknowledgments

R-*m*TFD-MPAB (99% pure) was a gift from Karol Bruzik (Department of Medicinal Chemistry and Pharmacognosy, Univerisity of Illinois, Chicago, IL). We thank Jonathan B. Cohen (Neurobiology Department, Harvard Medical School, Boston, MA) for helpful comments on the manuscript.

Authorship Contributions

Participated in research design: Szabo, Nourmahnad, Forman.
Conducted experiments: Szabo, Nourmahnad, Halpin.
Performed data analysis: Szabo, Nourmahnad, Forman.
Wrote or contributed to writing of the manuscript: Forman.

References

Baumann SW, Baur R, and Sigel E (2001) Subunit arrangement of γ-aminobutyric acid type A receptors. *J Biol Chem* **276**:36275–36280.
Belelli D, Lambert JJ, Peters JA, Wafford K, and Whiting PJ (1997) The interaction of the general anesthetic etomidate with the γ-aminobutyric acid type A receptor is influenced by a single amino acid. *Proc Natl Acad Sci USA* **94**:11031–11036.
Bevington PR and Robinson DK (2002) *Data Reduction and Error Analysis for the Physical Sciences*, 3rd ed, McGraw-Hill, New York.
Brohan J and Goudra BG (2017) The role of GABA receptor agonists in anesthesia and sedation. *CNS Drugs* **31**:845–856.
Cao LQ, Montana MC, Germann AL, Shin DJ, Chakrabarti S, Mennerick S, Yuede CM, Wozniak DF, Evers AS, and Akk G (2018) Enhanced GABAergic actions resulting from the coapplication of the steroid 3α-hydroxy-5α-pregnane-11,20-dione (alfaxalone) with propofol or diazepam. *Sci Rep* **8**:10341.
Chang Y and Weiss DS (1999) Allosteric activation mechanism of the $\alpha1\beta2\gamma2$ γ-aminobutyric acid type A receptor revealed by mutation of the conserved M2 leucine. *Biophys J* **77**:2542–2551.
Chiara DC, Jayakar SS, Zhou X, Zhang X, Savechenkov PY, Bruzik KS, Miller KW, and Cohen JB (2013) Specificity of intersubunit general anesthetic-binding sites in the transmembrane domain of the human $\alpha1\beta3\gamma2$ γ-aminobutyric acid type A ($GABA_A$) receptor. *J Biol Chem* **288**:19343–19357.
Desai R, Ruesch D, and Forman SA (2009) γ-Amino butyric acid type A receptor mutations at β2N265 alter etomidate efficacy while preserving basal and agonist-dependent activity. *Anesthesiology* **111**:774–784.
Feng HJ, Jounaidi Y, Haburcak M, Yang X, and Forman SA (2014) Etomidate produces similar allosteric modulation in $\alpha1\beta3\delta$ and $\alpha1\beta3\gamma2L$ $GABA_A$ receptors. *Br J Pharmacol* **171**:789–798.
Forman SA (2012) Monod-Wyman-Changeux allosteric mechanisms of action and the pharmacology of etomidate. *Curr Opin Anaesthesiol* **25**:411–418.
Forman SA (2018) Combining mutations and electrophysiology to map anesthetic sites on ligand-gated ion channels. *Methods Enzymol* **602**:369–389.
Forman SA and Miller KW (2016) Mapping general anesthetic sites in heteromeric γ-aminobutyric acid type A receptors reveals a potential for targeting receptor subtypes. *Anesth Analg* **123**:1263–1273.
Forman SA and Stewart D (2012) Mutations in the $GABA_A$ receptor that mimic the allosteric ligand etomidate. *Methods Mol Biol* **796**:317–333.
Germann AL, Shin DJ, Kuhrau CR, Johnson AD, Evers AS, and Akk G (2018) High constitutive activity accounts for the combination of enhanced direct activation and reduced potentiation in mutated $GABA_A$ receptors. *Mol Pharmacol* **93**:468–476.
Guitchounts G, Stewart DS, and Forman SA (2012) Two etomidate sites in $\alpha1\beta2\gamma2$ γ-aminobutyric acid type A receptors contribute equally and noncooperatively to modulation of channel gating. *Anesthesiology* **116**:1235–1244.
Jayakar SS, Zhou X, Chiara DC, Dostalova Z, Savechenkov PY, Bruzik KS, Dailey WP, Miller KW, Eckenhoff RG, and Cohen JB (2014) Multiple propofol-binding sites in a γ-aminobutyric acid type A receptor ($GABA_AR$) identified using a photoreactive propofol analog. *J Biol Chem* **289**:27456–27468.
Jayakar SS, Zhou X, Savechenkov PY, Chiara DC, Desai R, Bruzik KS, Miller KW, and Cohen JB (2015) Positive and negative allosteric modulation of an $\alpha1\beta3\gamma2$ γ-aminobutyric acid type A ($GABA_A$) receptor by binding to a site in the transmembrane domain at the γ^+-β^- interface. *J Biol Chem* **290**:23432–23446.
Krasowski MD, Koltchine VV, Rick CE, Ye Q, Finn SE, and Harrison NL (1998) Propofol and other intravenous anesthetics have sites of action on the γ-aminobutyric acid type A receptor distinct from that for isoflurane. *Mol Pharmacol* **53**: 530–538.
Li GD, Chiara DC, Sawyer GW, Husain SS, Olsen RW, and Cohen JB (2006) Identification of a $GABA_A$ receptor anesthetic binding site at subunit interfaces by photolabeling with an etomidate analog. *J Neurosci* **26**:11599–11605.
Li P, Bracamontes JR, Manion BD, Mennerick S, Steinbach JH, Evers AS, and Akk G (2014) The neurosteroid 5β-pregnan-3α-ol-20-one enhances actions of etomidate as a positive allosteric modulator of $\alpha1\beta2\gamma2L$ $GABA_A$ receptors. *Br J Pharmacol* **171**: 5446–5457.
Li P, Eaton MM, Steinbach JH, and Akk G (2013) The benzodiazepine diazepam potentiates responses of $\alpha1\beta2\gamma2L$ γ-aminobutyric acid type A receptors activated by either γ-aminobutyric acid or allosteric agonists. *Anesthesiology* **118**:1417–1425.
Maldifassi MC, Baur R, and Sigel E (2016) Functional sites involved in modulation of the $GABA_A$ receptor channel by the intravenous anesthetics propofol, etomidate and pentobarbital. *Neuropharmacology* **105**:207–214.
Mihic SJ, Ye Q, Wick MJ, Koltchine VV, Krasowski MD, Finn SE, Mascia MP, Valenzuela CF, Hanson KK, Greenblatt EP, et al. (1997) Sites of alcohol and volatile anaesthetic action on $GABA_A$ and glycine receptors. *Nature* **389**:385–389.
Nourmahnad A, Stern AT, Hotta M, Stewart DS, Ziemba AM, Szabo A, and Forman SA (2016) Tryptophan and cysteine mutations in M1 helices of $\alpha1\beta3\gamma2L$ γ-aminobutyric acid type A receptors indicate distinct intersubunit sites for four intravenous anesthetics and one orphan site. *Anesthesiology* **125**:1144–1158.
Olsen RW and Sieghart W (2009) $GABA_A$ receptors: subtypes provide diversity of function and pharmacology. *Neuropharmacology* **56**:141–148.
Phulera S, Zhu H, Yu J, Claxton DP, Yoder N, Yoshioka C, and Gouaux E (2018) Cryo-EM structure of the benzodiazepine-sensitive $\alpha1\beta1\gamma2S$ tri-heteromeric $GABA_A$ receptor in complex with GABA. *eLife* **7**:e39383.
Ruesch D, Neumann E, Wulf H, and Forman SA (2012) An allosteric coagonist model for propofol effects on $\alpha1\beta2\gamma2L$ γ-aminobutyric acid type A receptors. *Anesthesiology* **116**:47–55.
Rüsch D, Zhong H, and Forman SA (2004) Gating allosterism at a single class of etomidate sites on $\alpha_1\beta_2\gamma_{2L}$ $GABA_A$ receptors accounts for both direct activation and agonist modulation. *J Biol Chem* **279**:20982–20992.
Scheller M and Forman SA (2002) Coupled and uncoupled gating and desensitization effects by pore domain mutations in $GABA_A$ receptors. *J Neurosci* **22**:8411–8421.
Shin DJ, Germann AL, Covey DF, Steinbach JH, and Akk G (2019) Analysis of $GABA_A$ receptor activation by combinations of agonists acting at the same or distinct binding sites. *Mol Pharmacol* **95**:70–81.
Shin DJ, Germann AL, Johnson AD, Forman SA, Steinbach JH, and Akk G (2018) Propofol is an allosteric agonist with multiple binding sites on concatemeric ternary $GABA_A$ receptors. *Mol Pharmacol* **93**:178–189.
Shin DJ, Germann AL, Steinbach JH, and Akk G (2017) The actions of drug combinations on the $GABA_A$ receptor manifest as curvilinear isoboles of additivity. *Mol Pharmacol* **92**:556–563.
Siegwart R, Krähenbühl K, Lambert S, and Rudolph U (2003) Mutational analysis of molecular requirements for the actions of general anaesthetics at the γ-aminobutyric $acid_A$ receptor subtype, $\alpha1\beta2\gamma2$. *BMC Pharmacol* **3**:13.
Sigel E and Steinmann ME (2012) Structure, function, and modulation of $GABA_A$ receptors. *J Biol Chem* **287**:40224–40231.
Steinbach JH and Akk G (2019) Applying the Monod-Wyman-Changeux allosteric activation model to pseudo-steady-state responses from $GABA_A$ receptors. *Mol Pharmacol* **95**:106–119.
Stewart D, Desai R, Cheng Q, Liu A, and Forman SA (2008) Tryptophan mutations at azi-etomidate photo-incorporation sites on α_1 or β_2 subunits enhance $GABA_A$ receptor gating and reduce etomidate modulation. *Mol Pharmacol* **74**:1687–1695.
Ueno S, Lin A, Nikolaeva N, Trudell JR, Mihic SJ, Harris RA, and Harrison NL (2000) Tryptophan scanning mutagenesis in TM2 of the $GABA_A$ receptor α subunit: effects on channel gating and regulation by ethanol. *Br J Pharmacol* **131**:296–302.
Ueno S, Wick MJ, Ye Q, Harrison NL, and Harris RA (1999) Subunit mutations affect ethanol actions on $GABA_A$ receptors expressed in *Xenopus* oocytes. *Br J Pharmacol* **127**:377–382.
Walters RJ, Hadley SH, Morris KD, and Amin J (2000) Benzodiazepines act on $GABA_A$ receptors via two distinct and separable mechanisms. *Nat Neurosci* **3**: 1274–1281.
Ziemba AM and Forman SA (2016) Correction for inhibition leads to an allosteric co-agonist model for pentobarbital modulation and activation of $\alpha1\beta3\gamma2L$ $GABA_A$ receptors. *PLoS One* **11**:e0154031.

Address correspondence to: Dr. Stuart A. Forman, Department of Anesthesia Critical Care and Pain Medicine, Jackson 444, Massachusetts General Hospital, Boston, MA 02114. E-mail: saforman@mgh.harvard.edu

MOL # 115048

Supplemental Data

Title: **Monod-Wyman-Changeux Allosteric Shift Analysis in Mutant α1β3γ2L $GABA_A$ Receptors Indicates Selectivity and Cross-Talk Among Intersubunit Transmembrane Anesthetic Sites**

Authors: Andrea Szabo, Anahita Nourmahnad, Elizabeth Halpin, and Stuart A. Forman

Journal: Molecular Pharmacology

Supplemental Table S1

Non-Linear Least Squares Fitted Logistic Parameters from Figure 3

Receptor (n)	Fitted Parameter	GABA	GABA + ETO	GABA +MPAB	GABA + PRO
α1β3γ2L	P_{min} (SE)	0.00 (0.008)	0.00 (0.010)	0.03 (0.012)	0.01 (0.012)
(n ≥ 3)	P_{max} (SE)	0.87 (0.012)	1.00 (0.014)	0.99 (0.016)	0.98 (0.017)
	EC_{50} (μM) [95% CI]	59 [53 to 66]	4.1 [3.6 to 4.7]	3.3 [2.8 to 3.8]	4.0 [3.5 to 4.7]
	nH (SE)	1.16 (0.062)	1.00 (0.056)	1.10 (0.079)	1.21 (0.092)
α1S270Iβ3γ2L	P_{min} (SE)	0.020 (0.0089)	0.34 (0.059)	0.061 (0.0097)	0.05 (0.012)
(n ≥ 3)	P_{max} (SE)	0.78 (0.011)	0.96 (0.059	0.89 (0.011)	0.98 (0.017)
	EC_{50} (μM) [95% CI]	2.3 [2.1 to 2.6]	0.17 [0.06 to 0.45]	1.1 [0.98 to 1.3]	1.8 [1.5 to 2.2]
	nH (SE)	1.5 (0.11)	0.8 (0.30)	0.91 (0.053)	0.77 (0.049)
α1β3N265Mγ2L	P_{min} (SE)	0.00 (0.005)	0.00 (0.003)	0.02 (0.010)	0.00 (0.003)
(n ≥ 3)	P_{max} (SE)	0.72 (0.018)	0.73 (0.010)	0.96 (0.013)	0.74 (0.010)
	EC_{50} (μM) [95% CI]	118 [96 to145]	117 [103 to132]	11 [10 to 13]	96 [85 to108]
	nH (SE)	0.99 (0.079)	1.12 (0.062)	1.19 (0.075)	1.14 (0.062)
α1β3γ2LS280W	P_{min} (SE)	0.015 (0.0084)	0.15 (0.016)	0.01 (0.018)	0.014 (0.0073)
(n ≥ 3)	P_{max} (SE)	0.71 (0.017)	1.01 (0.030)	0.74 (0.072)	0.84 (0.015)
	EC_{50} (μM) [95% CI]	29 [24 to 35]	4.9 [3.6 to 6.6]	59 [24 to 144]	8.3 [7.1 to 9.7]
	nH (SE)	0.97 (0.076)	0.9 (0.11)	0.6 (0.10)	0.88 (0.051)
α1A291Wβ3γ2L	P_{min} (SE)	0.08 (0.032)	0.63 (0.018)	0.28 (0.019)	0.50 (0.035)
(n ≥ 3)	P_{max} (SE)	1.0 (0)	1.01 (0.018)	0.99 (0.016)	1.0 (0.012)
	EC_{50} (μM) [95% CI]	0.37 [0.27 to 0.52]	0.10 [0.06 to 0.17]	0.35 [0.26 to 0.49]	0.25 [0.13 to 0.51]
	nH (SE)	0.84 (0.087)	0.9 (0.15)	0.67 (0.064)	0.8 (0.16)
α1β3M286Wγ2L	P_{min} (SE)	0.05 (0.023)	0.07 (0.013)	0.50 (0.018)	0.09 (0.013)
(n ≥ 3)	P_{max} (SE)	1.0 (0)	1.0 (0)	1.0 (0)	1.0 (0)
	EC_{50} (μM) [95% CI]	5.9 [4.5 to 7.7]	4.0 [3.4 to 4.6]	1.7 [1.1 to 2.5]	4.6 [4.1 to 5.3]
	nH (SE)	0.77 (0.063)	0.79 (0.035)	1.0 (0.15)	1.00 (0.050)
α1β3γ2LS301W	P_{min} (SE)	0.05 (0.013)	0.17 (0.013)	0.101 (0.0050)	0.13 (0.010)
(n ≥ 3)	P_{max} (SE)	0.90 (0.029)	0.99 (0.021)	0.88 (0.013)	1.03 (0.019)
	EC_{50} (μM) [95% CI]	43 [32 to 58]	3.0 [2.4 to 3.9]	20 [18 to 23]	4.4 [3.6 to 5.3]
	nH (SE)	0.71 (0.060)	0.81 (0.073)	0.70 (0.028)	0.81 (0.053)

Fits are to Eq. 1 in Methods. ETO = 3.2 μM etomidate; MPAB = 8 μM R-mTFD-MPAB; PRO = 5 μM propofol

Table S2

Additive Allosteric Effects of M2 and M3 Mutations by Drug, Corrected for GABA Efficacy

			Δ[Log(d)-Log(c)] values ± sd		
	Mutations	**Log(c)**	**Etomidate**	**mTFD-MPAB**	**Propofol**
	Wild-Type	**-2.22 ± 0.0084**	**0.31 ± 0.075**	**0.09 ± 0.070**	**0.33 ± 0.070**
M2-15′	α1S270I	-1.18 + 0.024	0.71 ± 0.090	-0.67 ± 0.083	-0.41 ± 0.084
	β3N265M	-2.18 + 0.010	-1.84 ± 0.080	-0.60 ± 0.11	-1.76 ± 0.075
	γ2S280W	-1.15 ± 0.025	0.37 ± 0.090	-1.22 ± 0.085	-0.43 ± 0.083
	Sum		**-0.8 ± 0.15**	**-2.5 ± 0.16**	**-2.6 ± 0.14**
M3-36′	α1A291W	-1.03 + 0.026	0.50 ± 0.089	-0.45 ± 0.10	0.23 ± 0.093
	β3M286W	-1.14 + 0.034	-0.60 ± 0.13	-0.15 ± 0.090	-0.6 ± 0.12
	γ2S301W	-0.85 + 0.005	0.18 ± 0.093	-0.51 ± 0.088	-0.12 ± 0.095
	Sum		**0.1 ± 0.18**	**-0.8 ± 0.16**	**-0.3 ± 0.18**